

# 1 Temperature and nutrient availability influence radial growth of 2 *Picea abies* at opposite slopes in treeline ecotone

3 Hana Kuželová<sup>1</sup>, Tomáš Chuman<sup>1</sup>, Jelena Lange<sup>1</sup>, Jan Tumajer<sup>1</sup>, Václav Treml<sup>1</sup>

4 <sup>1</sup>Department of Physical Geography and Geoecology, Faculty of Science, Charles University, Albertov 6, 12800 Prague,  
5 Czech Republic

6 Correspondence to: Václav Treml (treml@natur.cuni.cz)

7 **Abstract.** Treeline ecotones in complex mountain landscapes are exposed to pronounced differences in irradiation and soil  
8 nutrient availability. Different amounts of nutrients and direct solar energy can influence tree stem growth especially in  
9 lower parts of treeline ecotone, where trees are still temperature limited, though located below the upper margin of tree life  
10 form. We hypothesized that at two sites located on north and south-facing slopes, differences in nutrient availability  
11 outperform temperature differences in modulating stem growth rates while growth phenology is driven by temperature  
12 seasonality. To test this hypothesis, we compared the growth phenology and kinetics of *Picea abies* in the lower part of  
13 treeline ecotone between a north-facing slope with relatively nutrient-rich soils and a south-facing slope with nutrient-poor  
14 soils. We analysed intra-annual wood formation, soil and air microclimate and soil and needle nutrient content. Our results  
15 showed that thermal differences between south and north-facing slopes are small but nontrivial involving higher daytime  
16 temperature at south-facing slopes and longer irradiation of north-facing slope during the middle part of growing season. The  
17 timing of growth onset and maximum growth rate were almost synchronized between both slopes. Accordingly, annual stem  
18 growth at both sites was most sensitive to the meteorological conditions at the start of the growing season and around the  
19 summer solstice. However, the absolute growth rate was higher on the north-facing slope, consistent with a higher  
20 availability and content of base cations in the soil and the needles. Our results suggest that temperature governs growth  
21 phenology at the lower part of the treeline ecotone, but nutrient availability modulates the growth rate in the peak season  
22 when temperature no longer limits cambial activity. We demonstrated that the effect of nutrient availability can be superior  
23 to the effect of slope aspect for stem growth rates of *Picea abies* located in the lower part of treeline ecotone in temperate  
24 mountain range.

## 25 1 Introduction

26 In cold environments, tree stem growth is tightly linked to temperature oscillations during the growing season (Rossi et al.,  
27 2016; Körner, 2021), which is reflected in the seasonal phenology of wood formation, that is, cambial division and xylem  
28 differentiation (Cuny et al., 2015). There are minimum temperature thresholds for both photosynthesis and the processes  
29 linked to the investment of non-structural carbohydrates into developing xylem, the latter being lower and thus representing

30 the ultimate limitation of stem growth (Fatichi et al., 2019). This is apparent along elevation transects where both non-  
31 structural carbohydrates and nutrient contents in twigs, leaves and sapwood increase towards the treeline as a result of  
32 increasing sink limitation of the growth (Hoch and Körner, 2012; Fajardo and Piper 2017; Doležal et al., 2019). While no  
33 exceptions from pure sink limitation of tree growth have been found for broadleaved treelines in the southern hemisphere  
34 (Fajardo and Piper 2017), some studies examining conifers in permafrost zone have highlighted the important role of nutrient  
35 availability in co-limiting stem growth (Sullivan et al., 2015; Dial et al., 2022). Although this is probably not generally valid  
36 for conifer treelines outside the permafrost zone (Hagedorn et al. 2020; Körner, 2021), the nutrient and moisture co-  
37 limitation of tree growth can play a role at local upper tree limits (boundaries of realized niche) or in the lower part of  
38 treeline ecotone, several tens to hundred meters below treeline (Möhl et al., 2018; Körner and Hoch, 2023). Such ecotones  
39 are common as current treelines often lag behind the pace of warming (Lu et al., 2021; Shi et al., 2022).

40 The low-temperature limit of tree growth at its cold range boundary is evidenced by growth resumption after exceeding a  
41 certain temperature threshold, as shown both by warming/cooling experiments (Gričar et al., 2006; Lenz et al.; 2013) and by  
42 observations in natural treeline settings (Körner and Hoch, 2006; Rossi et al., 2007). Indirectly, the prevailing low-  
43 temperature limitation of tree growth at cold sites is supported by similar thermal limits of global treelines (Körner and  
44 Paulsen, 2004). Furthermore, tree-ring chronologies from treelines are significantly correlated with growing season  
45 temperature (Chagnon et al., 2023), and calibrated thermal limits of wood formation models agree with those based on direct  
46 or experimental observations (Tumajer et al., 2021).

47 Recently, tree growth in cold biomes tends to accelerate in some areas, which has often been attributed to warming and an  
48 extension of the growing season (Shi et al., 2020; Li et al., 2023). However, in forest stands near treeline, observed growth  
49 enhancement has been connected to increased nitrogen supply in some regions (Kolář et al., 2015; Möhl et al., 2018; Etzold  
50 et al., 2020). Sullivan et al. (2015) showed better performance in shoot, stem and root growth at microsites relatively richer  
51 in nitrogen at the Arctic treeline due to warmer soils and a higher snowpack accelerating nutrient cycles (Dawes et al., 2017).  
52 Not only nitrogen (N) but also phosphorus (P, and namely the stoichiometry of N and P) was suggested as a limiting factor  
53 of tree occurrence at some treeline ecotone sites in the Himalayas (Müller et al., 2017). Apart from N and P, the role of other  
54 nutrients, especially base cations, has been largely neglected at tree stands near their cold distribution margins. Recently,  
55 there is a growing body of literature showing that base cations can play a vital role under certain conditions in limiting tree  
56 growth in the treeline ecotone (Drollinger et al., 2017) or in montane forests (Körner, 2022; Oulehle et al., 2023).

57 Local evidences of growth enhancements at sites relatively enriched by N and P are not necessarily in conflict with the  
58 ultimate role of low temperature limitation of tree growth at treeline (Körner, 2012) and with observations of increasing  
59 nutrient concentrations in leaves with elevation near cold margins of tree distribution (Fajardo and Piper, 2017). They rather  
60 suggest that nutrient availability together with low temperature might co-determine growth dynamics at upper tree limits  
61 whose position is not in equilibrium with current climate (Lu et al., 2021; Körner and Hiltbrunner, 2024).

62 In a complex mountain relief, a high variation in topoclimate and soil conditions can create a heterogenous mosaic of sites  
63 differing in local surface temperature (Jochner et al., 2017; Kuželová et al., 2021) as well as nutrient content (Liptzin et al.,

64 2013, Mayor et al., 2017). Probably the best-known topoclimatic effect is the so-called slope exposure phenomenon, which  
65 suggests that south-facing slopes in the northern hemisphere outside the tropics are warmer than north-facing slopes, and  
66 vice versa in the southern hemisphere (Körner, 2012). This phenomenon is less pronounced on forested slopes (Paulsen et  
67 al., 2001). Sites on opposite slopes might differ not only in insolation and surface temperature but also in nutrient  
68 availability, as surface temperature might influence litter decomposition through surface moisture and snow melt patterns  
69 (Dawes et al., 2017; Ellison et al., 2019; Stark et al., 2023).

70 In this study, we use an opposite slope aspect design in a complex research setting, which allows us to cover multiple site  
71 properties that potentially influence tree growth performance in the lower part of the treeline ecotone. This is a typical  
72 situation for the majority of current treelines which are located below physiological limit of tree existence because the pace  
73 of warming is much faster than upward shift of treeline (Lu et al., 2021). We carried out detailed observations of *Picea abies*  
74 trees in terms of intra-annual wood formation and inter-annual climate-growth responses together with analyses of site  
75 thermal and moisture properties and soil and foliar nutrient content. We test the general assumption that at the lower part of  
76 treeline ecotone, the crucial phases of tree growth, such as growth resumption and timing of the peak growth rate, are driven  
77 by thermal and solar constraints (Rossi et al., 2006b; Rossi et al., 2007). However, we hypothesize that the growth rate is  
78 influenced by nutrient availability, given the positive effect of nutrient availability on absolute tree growth that has been  
79 shown at some cold-limited sites (Möhl et al., 2018; Sullivan et al., 2015).

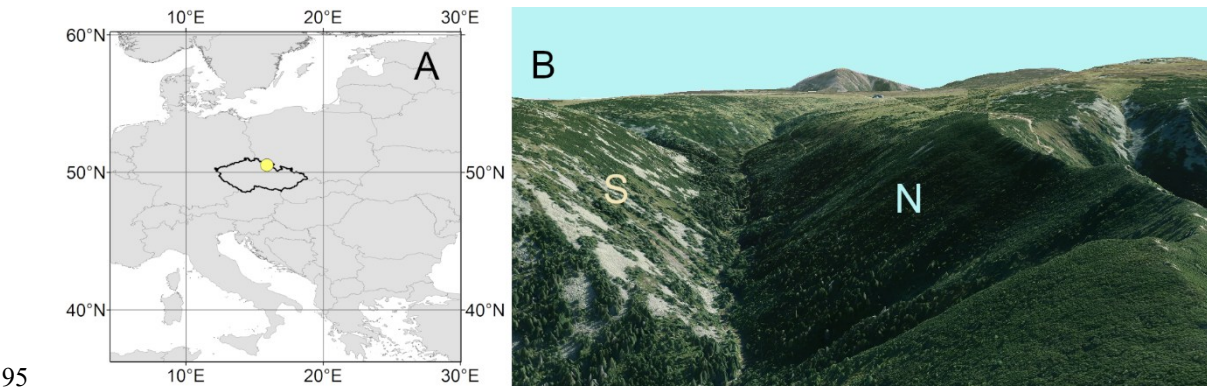
## 80 **2 Material and Methods**

### 81 **2.1 Study area**

82 Our study focuses on a dominant tree species of treeline ecotone *Picea abies* [L.] Karst. growing on N and S-slopes in the  
83 Krkonoše Mts, Czech Republic (50°43'N, 15°40'E, site elevation 1250 m a.s.l., Fig. 1). The Krkonoše Mts, with the highest  
84 peak Mt Sněžka (1602 m a.s.l.), are characterized by high annual precipitation sums (on average 1400–1600 mm) and a  
85 mean annual temperature of 0.5°C in the uppermost locations (Metelka et al., 2007). Snow cover in the treeline ecotone lasts  
86 from November until May, with a maximum snow depth of about 2 m (Metelka et al., 2007). The treeline ecotone is situated  
87 at elevations ranging from 1250 to 1450 m.

88 Two sites on opposite slopes (N-slope, S-slope) were established in the lower part of the treeline ecotone in the Bílé Labe  
89 valley (Fig. 1). The canopy cover at both sites was 20 %, and the tree height of adult individuals ranged between 8 and 13 m.  
90 *Picea abies* stands are gradually replaced by shrubland dominated by *Pinus mugo* in upslope direction. Both sites are located  
91 on steep slopes (inclination between 20° and 30°) with frequent patches of scree. The N-slope site is located on the  
92 transition between gneiss and mica-schist (upper part) and granodiorites (lower part). The S-slope site is underlaid by  
93 granites. Skeletic Leptosols and Skeletic Podzols are the dominant soil types on both slopes.

94



95 **Figure 1: (A) Location of the study area in Europe; (B) View from the west on the area with the south-facing (S) and north-facing (N) sites (modelled by ArcScene; ESRI, 2020).**

98 **2.2 Microclimatic monitoring**

99 We measured air and soil temperature and soil water potential to characterize site micro-climatic conditions from 2012 to  
100 2015 (to 2014 for soil water potential). Air temperature was recorded using sensors in radiation shields hanging in the tree  
101 crown approximately 7 m above the ground (one sensor at each site). Three sensors recorded the soil temperature and soil  
102 water potential of the root zone (mineral soil, -10 cm depth) at each site at places fully shaded by tree crowns. We used  
103 gypsum block soil water potential sensors to measure available soil moisture (measuring range 0 to -2 MPa, Delmhorst, EMS  
104 Brno). Air and soil temperatures and soil water potential were measured and stored at 1-hour intervals. Both air and soil  
105 temperature sensors have an accuracy of  $\pm 0.2^{\circ}\text{C}$  ([www.emsbrno.cz](http://www.emsbrno.cz)).

106 For each year and site, we calculated various variables that characterize the intra-annual meteorological patterns that are  
107 important for woody plants. Following Körner and Hiltbrunner (2018), we used soil temperature to define the duration of the  
108 meteorological growing season, i.e., the period when meteorological conditions potentially permit wood formation. We used  
109 the continuous period where soil temperature values were above  $3.2^{\circ}\text{C}$ , roughly corresponding to a mean weekly air  
110 temperature of  $0^{\circ}\text{C}$  (Körner and Paulsen, 2004). For both sites and for all years, we identified dates of the start, the end, and  
111 the duration of the meteorological growing season. Additionally, we computed mean air and soil temperature for the period  
112 June to September per site and year. Lastly, we calculated degree days by integrating all mean daily air temperatures  
113 exceeding  $5^{\circ}\text{C}$  for each site and year.

114 Site insolation was estimated using the ArcGIS Solar radiation tool (ESRI, 2020). Based on a digital elevation model with 5  
115 m resolution, we modelled the duration of direct insolation in hours and the solar irradiance ( $\text{W/m}^2$ ) for both sites and each  
116 day of the year. For each site, the insolation depended on the sun's position, slope aspect and inclination, and the location of  
117 surrounding ridges and peaks that shaded the sites for certain parts of the day and year.

118 **2.3 Soil and foliar nutrient analyses**

119 Soil samples were collected in two campaigns in October 2013 and October 2023. In the first campaign, we took two soil  
120 samples, and in the second campaign, we took three soil samples from the topmost 10 cm of the mineral soil at each site.  
121 Each sample from each campaign was pooled from five subsamples distributed randomly over each study site and properly  
122 mixed. Air-dried soils were sieved to remove the size fraction > 2 mm. Samples were analysed for exchangeable pH  
123 (CaCl<sub>2</sub>), cation exchange capacity (CEC), total soil N, soil organic carbon (Cox), and plant-available concentrations of Ca,  
124 Mg, K and P with Mehlich III extraction solution (Mehlich, 1984). Soil samples were analysed in the accredited laboratory  
125 of the Research Institute for Soil and Water Conservation, Prague. Differences between sites in measured soil variables were  
126 tested using the Kruskal-Wallis test implemented in R (R Development Core Team, 2023). For this purpose, we merged  
127 samples from both campaigns.

128 To compare the nutrient concentrations in needles between sites and to validate whether they reflect nutrient availability in  
129 soils, we collected current-year and previous-year needles from six trees at each site in October 2023. Sampled trees  
130 included those used for xylogenesis research. The long lag between the sampling of wood formation (2012-2014) and the  
131 sampling of foliar macroelements (2023) might influence absolute values of the determined elements because of their  
132 interannual variability, but not the difference between sites, which remains constant (Novotný et al., 2018). Branches from  
133 the upper part of the crown were cut using a telescopic long-reach pruner. Current- and previous-year needles were sampled  
134 from all cut branches and pooled per site. Pooled samples of 1000 current-year and 1000 previous-year needles were dried  
135 and then analysed for the content of main macro- and microelements. The analyses of the main macro- and microelements  
136 followed a standard ICP Forests protocol (Rautio et al., 2020). The foliage K, Ca, Mg and P was determined using ICP-OES  
137 after needle decomposition in a microwave oven. The total S and N content was analysed using the Leco CNS element  
138 analyser (Elementar Analysensysteme GmbH, Germany).

139

140 **2.4 Wood formation**

141 Six (2012) to eight trees (2013-2014) at each site were monitored in terms of wood formation (“xylogenesis”) over the three  
142 growing seasons (Table S1), which overlapped with the period of microclimatic measurements. A new set of healthy and  
143 dominant/co-dominant trees was selected for sampling each season to avoid possible impacts of previous year’s sampling on  
144 ongoing cambial activity. Wood microcores were sampled using a Trephor puncher (Rossi et al., 2006a) at a stem height of 1  
145 ± 0.2 m. Each sample contained the xylem of the current year, the cambial zone, the phloem, and one or more previous  
146 complete annual rings. The distance between adjacent sampling points on a stem was always greater than 3 cm to avoid  
147 effects of sampling on wood formation. Sampling intervals ranged from 7 to 10 days during the period from April to  
148 October, which significantly exceeds the typical duration of a growing season in a treeline environment (Treml et al., 2015).  
149 Once sampled, the microcores were immersed in a formaldehyde-ethanol-acetic acid fixative. The laboratory procedures

150 followed Gričar et al. (2006). The microcores were dehydrated using a successive series of ethanol and xylol-substitute and  
151 were then embedded in paraffin. 12-µm-thick cross sections were cut using a rotary microtome. The paraffin was removed,  
152 and samples were dehydrated using a successive series of xylol-substitute and ethanol solutions with descending/ascending  
153 ethanol concentrations. The cross sections were then stained with safranin and astra blue and mounted on permanent slides  
154 using Canada balsam.

155 The cells in the following wood phenological phases were counted for each cross section under 400–500x magnification  
156 using an optical microscope following Rossi et al. (2003): cells in the cambial zone, enlarging cells, wall-thickening cells,  
157 and mature cells. The number of cells in each developmental stage was counted in three radial files and subsequently  
158 averaged. The number of cells in the preceding tree ring was counted for three radial files and averaged. For each tree, the  
159 start and end date of each developmental phase (onset of cambial activity, enlarging phase, cell wall thickening phase,  
160 mature phase), and the overall duration of cambial activity were determined according to Rossi et al. (2007).

161 The counts of cells developed over the course of the growing season were fitted by a Gompertz function using the R package  
162 CAVIAR (Rathgeber et al., 2018). Next, the following parameters were determined from the Gompertz equation for each  
163 tree: the maximum daily cell production rate, the day of maximum cell production rate (both called critical dates, Rathgeber  
164 et al., 2018), and the mean daily production rate in the period when 90 % of cells were formed. Between-site differences of  
165 critical dates and production rates were tested using the Kruskal-Wallis test implemented in R (R Development Core Team,  
166 2023).

167 Logistic regressions were calculated to identify temperature thresholds at which the wood formation resumes (Rossi et al.,  
168 2008), with active/inactive wood formation as the explained binary variable and the 7-day backward mean soil and air  
169 temperature as explanatory variables. Only observations before the summer solstice were considered (Treml et al., 2019).  
170 The start of the active wood formation was alternatively defined by the occurrence of the first new cells in the cambial zone  
171 or the first enlarging cells. All calculations were performed in R (R Development Core Team, 2023).

## 172 **2.5 Climate-growth relationships of tree-ring chronologies**

173 Wooden cores were extracted at 1 m stem height from 45-50 randomly selected dominant and co-dominant individuals of  
174 *Picea abies* at each site in October 2013 using an increment borer (5 mm in diameter) (Table S3). Following standard  
175 laboratory procedures (fixation of cores to wooden supports, air-drying, sanding), tree-ring widths were measured using the  
176 WinDendro system (scanner and software with semi-automatic ring detection) (Regent Instruments, 2021). The resulting  
177 tree-ring series were visually and statistically cross-dated using PAST 5 software (Knibbe, 2013; Speer, 2010). We focused  
178 on high-frequency (interannual) growth variability preserved in tree-ring data. Therefore, tree-ring series were standardized  
179 with a cubic smoothing spline with a 40-year window length at a 50% frequency cutoff, and the autocorrelation was removed  
180 using autoregressive modelling (Cook and Peters, 1981). The residual tree-ring chronology for each site was built by  
181 averaging tree-ring series of individual trees. We calculated Pearson correlations between tree-ring chronologies and climatic  
182 time series with daily resolution and run the correlation analysis for time spans from ten to thirty consecutive days (Jevšenak,

183 2019). Daily climatic data (mean daily temperature, daily precipitation totals) from the nearest meteorological station  
184 Labská/Vrbatova bouda (1320 m a.s.l., 8 km westwards from our sites) were available and used from 1961 after filling data  
185 gaps using the neighbouring station. Before calculating correlations, temperature data were standardized in the same way as  
186 tree-ring data (Ols et al., 2023).

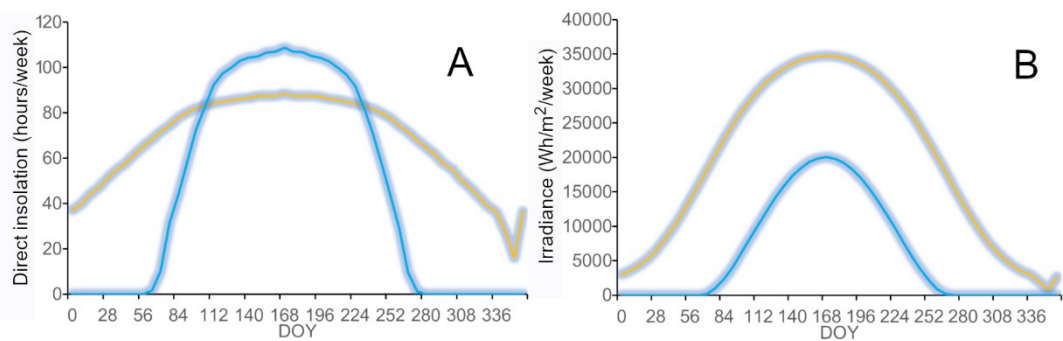
187 In order to characterize long-term growth rate, we converted tree-ring widths to basal area increments and calculated mean  
188 basal area increment for each tree (Speer, 2010). Mean basal area increments and their confidence intervals were then  
189 compared between sites considering tree age. Tree-ring and temperature data standardization and climate-growth correlations  
190 were performed using the dplR (Bunn et al., 2023) and dendroTools (Jevšenak and Levanič, 2018) R packages (R  
191 Development Core Team, 2023).

## 192 3 Results

### 193 3.1 Solar radiation and temperature differences

194 Irradiance was considerably higher on the S-slope than on the N-slope over the entire year (Fig. 2B). The N-slope was  
195 characterized by more than five months in winter without direct insolation (Fig. 2A). The duration of direct insolation was  
196 accordingly longer on the S-slope except for the period between end of April and mid-August when the weekly duration of  
197 insolation was longer on the N-slope, reflecting the effect of the complex topographical setting (Fig. 1B). Mean air  
198 temperature during the main growing season (June-September) was about 0.1 °C higher at the S-slope in most years, but this  
199 difference was smaller than the measurement error (Table 1, Fig. 3). Similarly, degree days were slightly higher at the S-  
200 slope (Table 1). Interestingly, differences in air temperature during the main part of the growing season showed a  
201 pronounced daily pattern with a warmer S-slope during the day and a warmer N-slope at night (Fig. 3D).

202



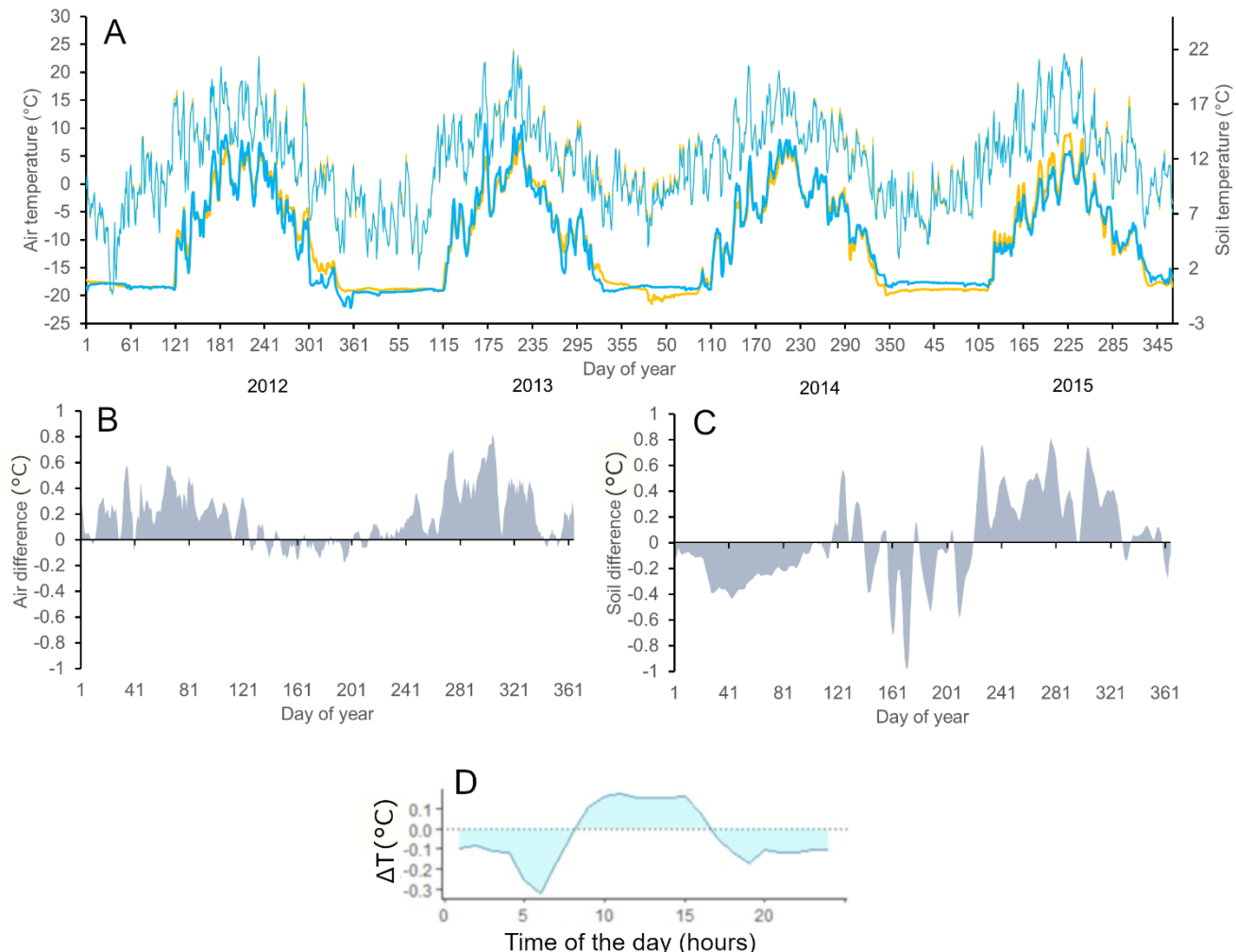
203  
204 **Figure 2: Modelled duration of direct insolation (A) and irradiance (B) plotted against the day of year (DOY) on the north-facing**  
205 **(blue) and south-facing (orange) sites.**

206

207 At both sites, soil temperature oscillated under the snowpack close to 0°C usually until the day of year (DOY) 110-120 (ca.  
208 end of April) and then abruptly increased (Fig. 3A). Soils tended to be cooler on the S-slope during the winter, possibly due  
209 to deeper freezing under a thinner snowpack. Soil temperature was higher on the S-slope at the very beginning and towards  
210 the end of the growing season, while soils on the N-slope tended to be warmer in the peak growing season (Fig. 3C), which  
211 roughly corresponds to the period when daily direct insolation is longer on the N-slope (Fig. 2A). As a result, mean soil  
212 temperature was slightly warmer (0.2-0.3 °C) at the N-slope over the June-September period in most years, with differences  
213 again being close to the measurement error, except in 2015 when the S-slope was substantially warmer (Table 1). There was  
214 no systematic pattern in the duration of the meteorologically-defined growing season (Table 1).

215 Both sites exhibited several periods with significant negative soil water potentials (Fig. S1), occurring mostly in the summers  
216 of 2013 (both N- and S-slope) and 2014 (N-slope) but also in the winters of 2012 (N-slope) and 2014 (S-slope).

217



218

219 **Figure 3: (A) Daily means of soil (bold lines, bottom) and air temperature (thin lines, top) for the north- (blue) and south- (orange)**  
220 **facing slope for the period 2012-2015. (B) Differences between south- and north-facing slopes (temperature south minus**  
221 **temperature north) smoothed by a 5-day moving average 2012 – 2015 for mean daily air temperature and (C) the same for mean**  
222 **daily soil temperature. (D) Differences in the course of daily air temperature (temperature south – temperature north; hourly**  
223 **interval) for June-August 2012-2015.**

224

225 **Table 1: Thermal characteristics of the growing season on the north (N-slope) and south-facing (S-slope) site calculated based on**  
226 **on-site measurements.**

Year	Site	Growing season duration (days)	Mean Air T in June – September (°C)	Mean Soil T in June – September (°C)	Degree days exceeding 5 °C
2012	N-slope	145	11.26	9.96	1023
	S-slope	167	11.34	9.81	1054
2013	N-slope	192	10.88	9.57	906
	S-slope	192	10.99	9.32	929
2014	N-slope	189	11.14	9.78	978
	S-slope	158	11.05	9.48	987
2015	N-slope	195	12.09	8.81	1036
	S-slope	196	12.18	9.59	1062
Mean ( $\pm$ SD)	N-slope	180 $\pm$ 20	11.3 $\pm$ 0.4	9.5 $\pm$ 0.4	985 $\pm$ 50
	S-slope	178 $\pm$ 16	11.4 $\pm$ 0.5	9.6 $\pm$ 0.2	1008 $\pm$ 54

227

### 228 **3.2 Nutrient content in soil and foliage**

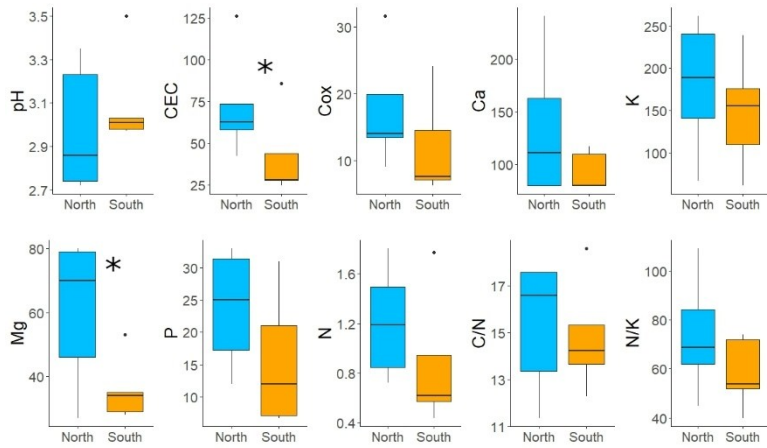
229 Soils at both sites were strongly acid with low CEC, P content and plant-available base cations except for K (Fig. 4, Table  
230 S2). The concentrations of base cations were systematically higher on the N-slope than on the S-slope. Statistically  
231 significant differences were detected for CEC and Mg ( $p<0.05$ , Fig. 4). The concentration of Ca was below the detection  
232 limit for half of the samples. The content of Cox and N was high, with a favourable C/N ratio at both sites.

233 In line with soil nutrient analysis, foliar macroelements were higher on the N-slope than on the S-slope both in current- and  
234 previous-year needles (Table 2). For the current-year needles, the concentrations of base cations (Ca, K, Mg) were about 25-  
235 29% higher on the N-slope. The content of P and N was also substantially (16-21%) higher on the N-slope (Table 2).

236

237

238



239

240 **Figure 4: Differences in soil characteristics between south- (orange) and north-facing (blue) slopes. Variables: exchangeable pH,**  
 241 **cation exchange capacity (CEC) (mol+/100g), soil organic carbon (Cox) (%), plant-available concentrations of Ca, Mg, K, P with**  
 242 **Mehlich III extraction solution (mg/kg), total soil N (%), and ratios of C/N and N/K. The analytical results for Ca that were below**  
 243 **the detection limit were replaced by 4/5 of the detection limit. Asterisks denote statistically significant differences.**

244 **Table 2: Foliar nutrients in mg/kg of dry matter. Samples were pooled from six trees at each site.**

Sample	Ca	K	Mg	P	N <sub>total</sub>	S <sub>total</sub>
<b>N-slope current year</b>	3944	7059	1177	1456	1.54	1040
<b>S-slope current year</b>	2785	5248	849	1213	1.32	833
<b>N-slope previous year</b>	4954	5913	1064	1245	1.64	1125
<b>S-slope previous year</b>	4608	4650	898	1039	1.31	887

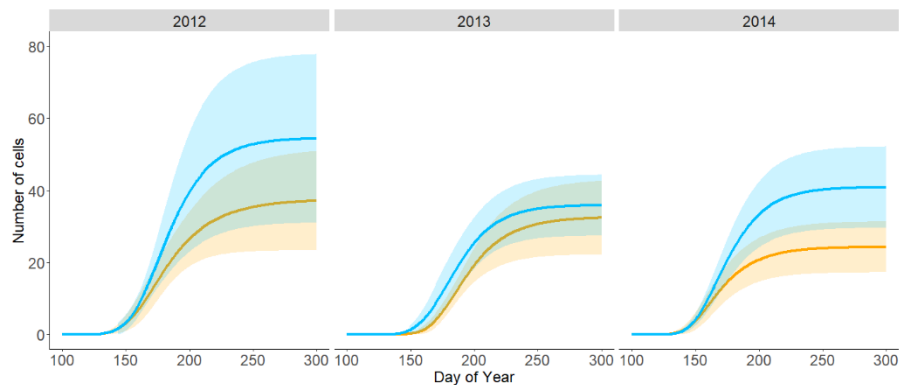
245

### 246 **3.3 Wood formation**

247 The N-slope exhibited a higher number of newly formed cells each year, with the greatest difference compared to the S-slope  
 248 found in 2014 (Fig. 5, Fig. S2). Although the difference was systematic across years and all parts of the growing season, it  
 249 was statistically non-significant due to the limited number of sampled trees and natural between-tree variability in  
 250 xylogenesis. The higher number of cells on the N-slope resulted from consistently higher mean and maximum cell formation  
 251 rates, i.e., faster stem growth; the difference was statistically significant in 2014 ( $p<0.05$ ) (Fig. 5, Fig. S3). Note that while  
 252 the tree age distribution was comparable between sites in 2012 and 2014, trees on the N-slope were about 50 years older in  
 253 2013 (Table S1).

254 Critical dates of wood formation, such as dates of the beginning, peak and end of wood formation did not show any  
 255 consistent pattern, and no difference was statistically significant (Fig. S3). The variability in critical dates among trees on the  
 256 S-slope was usually higher than on the N-slope. Similarly to critical dates derived from the Gompertz equation, there were

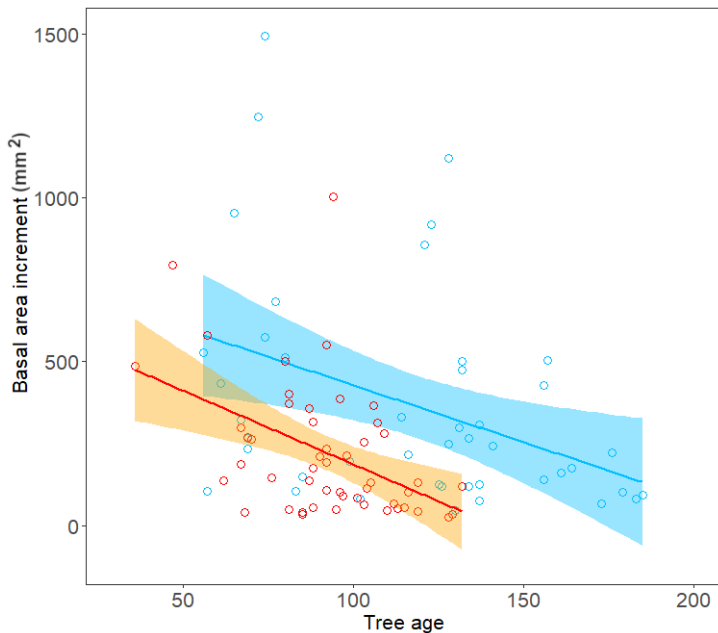
257 no consistent differences in dates of cell phenological phases between sites based on raw cell development data (Fig. S4).  
258 The duration of cell wall thickening was significantly longer on the N-slope in 2013 and 2014.  
259 Logistic regressions with growth resumption indicated by the first enlarging cells (binary response variable) and soil  
260 temperature (predictor) better fitted the data than regressions with cambial division (active/inactive - binary response  
261 variable) and air temperature (predictor) (Fig. S5). Growth onset represented by the occurrence of the first cambial cells  
262 occurred at 3.3 and 3.9 °C soil temperature and 3.6°C and 4.5°C air temperature on the S-slope and N-slope, respectively. In  
263 contrast, thresholds for the first enlarging cells were very similar at both sites and occurred at 4.7 °C of soil temperature at  
264 both sites and 6.4°C and 6.3°C of air temperature on the S-slope and N-slope, respectively.  
265



266  
267 **Figure 5: Number of tracheids in the newly developing annual tree ring for 2012-2014 for the north- (blue) and the south-facing**  
268 **(orange) site. Graphs show data fitted by the Gompertz function. Buffers denote 95 % confidence intervals.**

### 269 **3.4 Tree-ring width chronologies and their climate response**

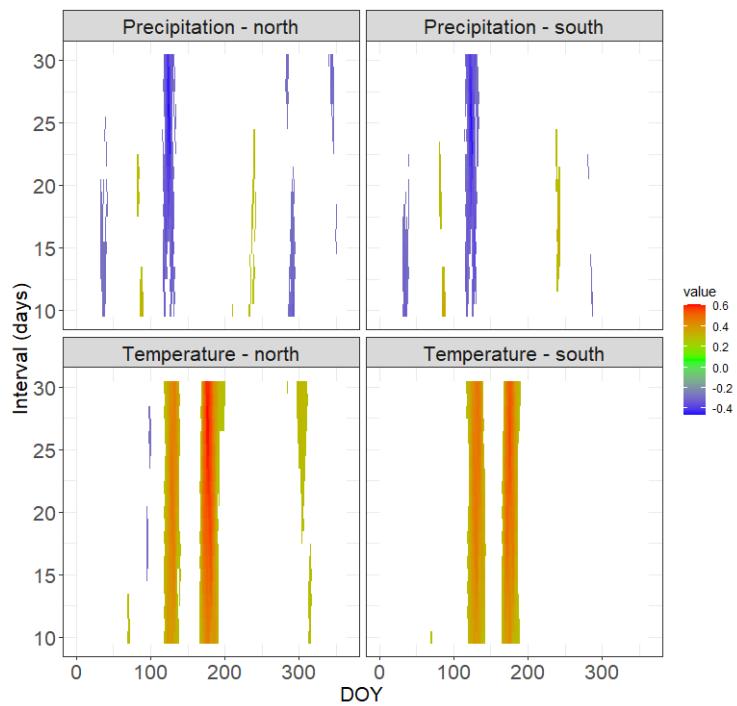
270 Tree-ring chronologies from both sites share their high-frequency variability (Fig. S6). Tree-ring series from south-facing  
271 slope are generally younger, the chronology characteristics such as mean sensitivity and expressed population signal are  
272 similar (Table S3). Mean basal area increments are significantly larger at the N-slope than at the S-slope (Fig. 6) consistently  
273 with the higher cell formation rates at the N-slope (Fig. 5). Both sites showed two prominent periods with significant  
274 temperature-growth correlations, indicating crucial parts of the season for annual ring width formation – the beginning of the  
275 growing season centered around DOY 125 (first week of May) and the peak growing season centered around DOY 180 (end  
276 of June, Fig. 7). Positive temperature-growth correlations were slightly stronger on the N-slope, with the maximum  
277 correlation coefficient exceeding 0.6 for a 25-day period centered around DOY 179. There was a significant negative  
278 correlation of growth at both sites with precipitation centered around DOY 115-125, which overlaps the positive effect of  
279 temperature at the beginning of the growing season (Fig. 7). The remaining significant climate-growth correlations are  
280 restricted to very short periods and might be stochastic.



281

282 **Figure 6: Relationship between mean tree basal area increment ( $\text{mm}^2$ ) and tree age for trees growing on the north-facing site  
283 (blue) and the south-facing site (orange).**

284



285

286 **Figure 7: Climate-growth correlations for tree-ring width chronologies of the north and south-facing site calculated over the**  
287 **period 1961-2013. Only statistically significant correlations are shown. The time window is centred over the respective days of the**  
288 **year (DOY). The y-axis shows the length of the window of the number of consecutive days for which the correlations were**  
289 **computed. Tree-ring chronologies are shown in Fig. S6.**

290 **4 Discussion**

291 We present a study that combines observations of radial stem growth at weekly temporal resolution with the analysis of sub-  
292 daily local microclimate and site nutrient availability at cold sites located at the lower part of the treeline ecotone about 150  
293 m below the local tree maxima. We found that phenological dates, particularly the onset of wood formation, as well as radial  
294 growth in relative terms, were strongly temperature-limited at both sites as expected, but the absolute growth rate was higher  
295 on the N-slope than on the S-slope. This is in line with our finding that soils were considerably richer in nutrients on the N-  
296 slope, which was also warmer than the S-slope during the nighttime.

297

298 **4.1 Thermal and nutrient limitation of growth**

299 We expected to find either the same thermal conditions within tree patches on both slopes or a slightly warmer S-slope  
300 (Paulsen et al., 2001), leading to similar growth onset, duration, and a similar growth rate. However, while we did find that  
301 both sites showed similar thermal conditions and thus similar constraints and timing of beginning and peak growth phases,  
302 the N-slope exhibited a systematically higher seasonal growth rate, albeit significant only in 2014. Consistently, significantly  
303 higher basal area increments were observed for trees growing on the N-slope than on the S-slope.

304 Tree growth at cold sites has been considered predominantly as low temperature-limited (Babst et al., 2019). Accordingly,  
305 we found clear support for the thermal limitation hypothesis as our temperature thresholds for growth resumption were very  
306 similar at both sites (between 3.3°C and 6.4°C depending on the temperature variable) and similar to the values published  
307 elsewhere (Rossi et al., 2007; Körner, 2021). Furthermore, radial stem growth at both sites, expressed as annual tree-ring  
308 width, showed very high sensitivity to variations in temperature during the identical periods of the year. Ring-width  
309 chronologies correlated with temperature mainly during the beginning of the growing season in early May, which is  
310 indicative for the onset of growth in the early growing season (Castagneri et al., 2017; Carrer et al., 2017; Li et al., 2023). In  
311 the same part of the season, tree-ring chronologies displayed negative correlations with precipitation. Precipitation usually  
312 falls in the form of snow at that time and delays the onset of the growing season. The second period with a significantly  
313 positive response of radial growth to temperature is the peak growing season at the end of June, when the rates of cell  
314 division and enlargement culminate (Castagneri et al., 2017; Rossi et al., 2006b). Our data thus show, that the timing of  
315 growth resumption and the peak rate of cell production are strongly constrained by temperature.

316 Notably, irrespective of the similar thermal constraints of stem growth on both slopes, the absolute production rate of new  
317 tracheids was always higher on the N-slope. Differences between sites were not significant at the 5% probability level except  
318 2014, probably due to the limited number of sampled trees, though similar or higher in our study than what is a common  
319 standard in wood formation studies (Cuny et al., 2015; Huang et al., 2021). Cell counts were higher each year on the N-  
320 slope, consistent with significantly higher stem growth over the entire lifespan of trees on the N-slope compared to the S-  
321 slope (Fig. 6). Factors responsible for the observed differences in growth rate could generally include differences in  
322 microclimate, tree age (Rathgeber et al., 2011; Zeng et al., 2017) or accessibility of nutrients (Drollinger et al., 2017). Tree  
323 age did not differ between sites in the years with the greatest differences in cell counts (2012, 2014). In 2013 trees were  
324 significantly older on the N-slope than on the S-slope. However, we still observed greater number of newly formed cells on  
325 the N-slope contrary to theoretical expectation as older trees usually form less cells than younger trees (Lundqvist et al.,  
326 2018).

327 It is unclear to what extent microclimatic differences were decisive in our study since we found between-site thermal  
328 differences within or close to the measurement error of the thermistors. The S-slope tended to be slightly more favourable  
329 with respect to air temperature and degree day sums. However, the N-slope was warmer during the night when stem water  
330 potentials are highest with intense cell expansion and division (Zweifel et al., 2021), which may thus benefit stem growth  
331 there. Differences in soil temperature were ambiguous: the S-slope tended to be warmer than the N-slope at the beginning of  
332 the growing season, but the N-slope was warmer during the peak growing season, leading to slightly warmer soils on N-  
333 slope for the June-September period. Only in the warmest year of the measurement period (2015), the S-slope was  
334 substantially warmer.

335 Overall, our temperature measurements showed that a part of the growing season was characterized by air and soil  
336 temperature well above the growth-limiting threshold of  $>5^{\circ}\text{C}$  (Körner, 2021), potentially allowing for the influence of other  
337 growth-limiting factors. One plausible explanation for the observed growth differences could thus be nutrient availability.  
338 Specifically, we suggest the better growth performance of trees at the N-slope may be due to a higher availability of base  
339 cations and perhaps also P, as can be seen from nutrient concentrations measured both in soils and in needles. Higher  
340 concentrations of leaf macronutrients at N-slope could also potentially indicate greater sink limit of growth (Hoch and  
341 Körner, 2012; Fajardo and Piper, 2017). However, in the light of higher growth rates and concentrations of macronutrients in  
342 soils of the N-slope, we interpret this pattern as a consequence of higher uptake of nutrients reflected in the source-driven  
343 higher growth rate (Ellison et al., 2019).

344 Not surprisingly, in an ecosystem saturated with N (Novotný et al., 2018), the main between-site differences cannot be  
345 attributed to N availability but to other nutrients such as Ca, Mg, or P. This applies especially to very acid soils with a pH of  
346 around 3, as in our case, where leaching of basal cations is likely (Lucas et al., 2011). In environments rich in C and N,  
347 stoichiometric requirements for building new biomass make other nutrients limiting, especially base cations and P (Mellert  
348 and Ewald, 2014; Norby et al., 2022; Körner, 2022). So far, most studies accentuated N availability as an important  
349 constraint of the growth performance of trees at cold sites (Möhl et al., 2018; Gustafson et al., 2021), but these studies

350 focused on ecosystems not saturated with N. The important role of P for tree growth has also been shown in forest  
351 ecosystems near their cold margin (Hagedorn et al., 2020; Ellison et al., 2019). Consistent with the traditional Liebig's law  
352 of the minimum (Liebig, 1840), our study highlights the importance of general stoichiometric principles of nutrient  
353 requirements for the production of new biomass, which may also play a crucial role in the growth rate of trees at cold sites.  
354 The source of the higher nutrient content in soils of our N-slope is not entirely clear. Metamorphic rocks prevalent on the  
355 north-facing slope are generally richer in Mg, Ca and K than granites prevalent on the S-slope, while the content of P is  
356 comparable between metamorphites and granites (Czech Geological Survey, 2024). Additionally to weathering, higher  
357 nighttime temperatures and slightly higher soil temperatures in the peak growing season on the N-slope may have enhanced  
358 decomposition rates and thus indirectly growth performance. Similar relationships between higher soil temperatures, higher  
359 soil nutrient content, and enhanced tree growth have been observed at subarctic treeline ecotones (Sullivan et al., 2015; Dial  
360 et al., 2024).

361

## 362 **4.2 Implications for tree growth in topographically complex cold landscapes**

363 Our data generally support the idea that the thermal differences between high-elevation slopes under forest cover are  
364 relatively subtle in the temperate zone (Paulsen and Körner, 2001; Treml and Banaš, 2008, Rita et al., 2021). Additionally,  
365 we would like to highlight two striking patterns related to our N-slope and S-slope sites that may be generalizable. First, the  
366 duration of direct sunlight during the growing season was longer on the N-slope, probably due to incoming morning and  
367 evening sunlight from the northeast and northwest, respectively. This phenomenon might increase with increasing latitudes  
368 and be stronger at less steeper slopes. An extreme example is the midnight irradiation of north-facing slopes beyond the  
369 polar circle (Kirchhefer, 2000). Second, probably as a consequence, nighttime air temperature was higher on the N-slope  
370 compared to the S-slope, leading to equal mean daily air temperature on both sites (the S-slope was warmer during the  
371 warmest part of the day). However, since the differences in night temperature were rather high, topographical effects on local  
372 air masses ventilation resulting in relatively lower radiative cooling on the N-slope than on the S-slope should also be  
373 considered in our case (Barry et al., 1992). Higher nighttime air temperature on the N-slope may also be the cause of warmer  
374 soils in some years but with differences close to the measurement error. We conclude that the thermal differences between  
375 tree stands growing on supposedly warmer, more growth-favorable south-facing slopes and cooler north-facing slopes can be  
376 so subtle that they may be overridden by local topography with related relief shading and local circulation.

377 Faster growth of trees on soils richer in nutrients also implies that the advance of current upper tree limits might be faster on  
378 fertile soils because seedlings could potentially reach a mature and reproductive age earlier (Dial et al., 2022). This remains  
379 to be rigorously tested, although some studies have already suggested greater potential for treeline advancement on fertile  
380 soils (Rousi et al., 2018; Gustafson et al., 2021).

381

382 **Conclusions**

383 We demonstrated that in the lower part of treeline ecotone in temperate mountains, thermal differences between south-facing  
384 and north-facing slopes can be subtle and may be overridden by relief shading and local air circulation. Crucial phases of  
385 stem growth, particularly the onset of wood formation and timing of peak growth rate, were constrained by temperature and  
386 day length. Consequently, phenology of wood formation was similar between slopes. However, the absolute growth rate was  
387 systematically higher on the north-facing slope with soils considerably enriched by nutrients. Our results suggest a joint  
388 effect of nutrient-driven absolute growth rate together with the thermally constrained growth phenology at sites close to the  
389 cold range limit of trees. These findings are essential for understanding stem growth trends at treelines whose current  
390 position often lags behind the pace of warming.

391

392 **Code and Data availability**

393 The data used for the analyses together with R scripts are available here: [10.5281/zenodo.14619874](https://doi.org/10.5281/zenodo.14619874)

394 **Supplement**

395 This article is accompanied by supplementary material.

396

397 **Author contributions**

398 HK and VT conceptualized the study. HK, and VT performed data processing. TCh and JT contributed to data analyses. HK  
399 and VT lead the paper writing. JL, TCh and JT contributed to paper writing (comments and revisions).

400

401 **Competing interests**

402 The authors declare no competing interests.

403 **Special issue statement**

404 This article is part of the special issue “Treeline ecotones under global change: linking spatial patterns to ecological  
405 processes”.

406 **Acknowledgements**

407 We appreciate the authority of the Krkonoše National Park for the permission to conduct research and for the logistical  
408 support. We further thank Jakub Kašpar and Šárka Zákravská for their help with fieldwork. We are grateful to two  
409 anonymous reviewers for their constructive comments to the earlier version of the manuscript.

410 **Financial support**

411 This study was funded by the Czech Science Foundation, grant number 22-26519S. H.K., V.T., J.L. and J.T. were supported  
412 by the Johannes Amos Comenius Programme (P JAC), project No. CZ.02.01.01/00/22\_008/0004605, Natural and  
413 anthropogenic georisks.

414 **References**

415 Babst, F., Bouriaud, O., Poulter, B., Trouet, V., Girardin, M. P. and Frank, D. C.: Twentieth century redistribution in  
416 climatic drivers of Global Tree Growth, *Science Advances*, 5(1), doi:10.1126/sciadv.aat4313, 2019.

417 Barry, R. G.: *Mountain Weather and climate*, Cambridge University Press, Cambridge, United Kingdom., 2008.

418 Bunn, A., Korpela, M., Biondi, F., Campelo, F., Mérian, P., Qeadan, F., Zang, C.: *dplR: Dendrochronology Program Library*  
419 in R. R package version 1.7.4, URL <https://CRAN.R-project.org/package=dplR>, 2022.

420 Carrer, M., Castagneri, D., Prendin, A. L., Petit, G. and von Arx, G.: Retrospective analysis of wood anatomical traits  
421 reveals a recent extension in tree cambial activity in two high-elevation conifers, *Frontiers in Plant Science*, 8,  
422 doi:10.3389/fpls.2017.00737, 2017.

423 Castagneri, D., Fonti, P., von Arx, G. and Carrer, M.: How does climate influence xylem morphogenesis over the growing  
424 season? insights from long-term intra-ring anatomy in *Picea abies*, *Annals of Botany*, doi:10.1093/aob/mcw274, 2017.

425 Chagnon, C., Moreau, G., D'Orangeville, L., Caspersen, J., Labrecque-Foy, J.-P. and Achim, A.: Strong latitudinal gradient  
426 in temperature-growth coupling near the treeline of the Canadian Subarctic Forest, *Frontiers in Forests and Global*  
427 *Change*, 6, doi:10.3389/ffgc.2023.1181653, 2023.

428 Cuny, H. E., Rathgeber, C. B., Frank, D., Fonti, P., Mäkinen, H., Prislan, P., Rossi, S., del Castillo, E. M., Campelo, F.,  
429 Vavrčík, H., Camarero, J. J., Bryukhanova, M. V., Jyske, T., Gričar, J., Gryc, V., De Luis, M., Vieira, J., Čufar, K.,  
430 Kirdyanov, A. V., Oberhuber, W., Treml, V., Huang, J.-G., Li, X., Swidrak, I., Deslauriers, A., Liang, E., Nöjd, P.,  
431 Gruber, A., Nabais, C., Morin, H., Krause, C., King, G. and Fournier, M.: Woody biomass production lags stem-girth  
432 increase by over one month in coniferous forests, *Nature Plants*, 1(11), doi:10.1038/nplants.2015.160, 2015.

433 Czech Geological Survey: Lithogeochemical database of the Czech Geological Survey. Czech Geological Survey. URL  
434 <http://www.geology.cz/litogeochemie>, 2024.

435 Dawes, M. A., Schleppi, P., Hättenschwiler, S., Rixen, C. and Hagedorn, F.: Soil warming opens the nitrogen cycle at the  
436 Alpine Treeline, *Global Change Biology*, 23(1), 421–434, doi:10.1111/gcb.13365, 2016.

437 Dial, R. J., Maher, C. T., Hewitt, R. E. and Sullivan, P. F.: Sufficient conditions for rapid range expansion of a boreal  
438 conifer, *Nature*, 608(7923), 546–551, doi:10.1038/s41586-022-05093-2, 2022.

439 Dial, R. J., Maher, C. T., Hewitt, R. E., Wockenfuss, A. M., Wong, R. E., Crawford, D. J., Zietlow, M. G. and Sullivan, P.  
440 F.: Arctic sea ice retreat fuels Boreal Forest Advance, *Science*, 383(6685), 877–884, doi:10.1126/science.adh2339, 2024.

441 Dolezal, J., Kopecky, M., Dvorsky, M., Macek, M., Rehakova, K., Capkova, K., Borovec, J., Schweingruber, F., Liancourt,  
442 P. and Altman, J.: Sink limitation of plant growth determines tree line in the arid Himalayas, *Functional Ecology*, 33(4),  
443 553–565, doi:10.1111/1365-2435.13284, 2019.

444 Drollinger, S., Müller, M., Kobl, T., Schwab, N., Böhner, J., Schickhoff, U. and Scholten, T.: Decreasing nutrient  
445 concentrations in soils and trees with increasing elevation across a treeline ecotone in Rolwaling Himal, Nepal, *Journal of*  
446 *Mountain Science*, 14(5), 843–858, doi:10.1007/s11629-016-4228-4, 2017.

447 Ellison, S. B., Sullivan, P. F., Cahoon, S. M. and Hewitt, R. E.: Poor nutrition as a potential cause of divergent tree growth  
448 near the Arctic treeline in Northern Alaska, *Ecology*, 100(12), doi:10.1002/ecy.2878, 2019.

449 ESRI: ArcGIS Desktop: Release 10.7.1. Redlands, Environmental Systems Research Institute, CA., 2020.

450 Etzold, S., Ferretti, M., Reinds, G. J., Solberg, S., Gessler, A., Waldner, P., Schaub, M., Simpson, D., Benham, S., Hansen,  
451 K., Ingerslev, M., Jonard, M., Karlsson, P. E., Lindroos, A.-J., Marchetto, A., Manninger, M., Meesenburg, H., Merilä,  
452 P., Nöjd, P., Rautio, P., Sanders, T. G. M., Seidling, W., Skudnik, M., Thimonier, A., Verstraeten, A., Vesterdal, L.,  
453 Vejpustkova, M. and de Vries, W.: Nitrogen deposition is the most important environmental driver of growth of pure,  
454 even-aged and managed European forests, *Forest Ecology and Management*, 458, 117762,  
455 doi:10.1016/j.foreco.2019.117762, 2020.

456 Fajardo, A. and Piper, F. I.: An assessment of carbon and nutrient limitations in the formation of the southern Andes Tree  
457 Line, *Journal of Ecology*, 105(2), 517–527, doi:10.1111/1365-2745.12697, 2016.

458 Fatichi, S., Pappas, C., Zscheischler, J. and Leuzinger, S.: Modelling carbon sources and sinks in terrestrial vegetation, *New*  
459 *Phytologist*, 221(2), 652–668, doi:10.1111/nph.15451, 2018.

460 Gričar, J., Zupančič, M., Čufar, K., Koch, G., Schmitt, U. and Oven, P.: Effect of local heating and cooling on cambial  
461 activity and cell differentiation in the stem of Norway spruce (*Picea abies*), *Annals of Botany*, 97(6), 943–951,  
462 doi:10.1093/aob/mcl050, 2006.

463 Gustafson, A., Miller, P. A., Björk, R. G., Olin, S. and Smith, B.: Nitrogen restricts future sub-arctic treeline advance in an  
464 individual-based dynamic vegetation model, *Biogeosciences*, 18(23), 6329–6347, doi:10.5194/bg-18-6329-2021, 2021.

465 Hagedorn, F., Dawes, M. A., Bubnov, M. O., Devi, N. M., Grigoriev, A. A., Mazepa, V. S., Nagimov, Z. Y., Shiyatov, S. G.  
466 and Moiseev, P. A.: Latitudinal decline in stand biomass and productivity at the elevational treeline in the Ural  
467 Mountains despite a common thermal growth limit, *Journal of Biogeography*, 47(8), 1827–1842, doi:10.1111/jbi.13867,  
468 2020.

469 Hansson, A., Dargusch, P. and Shulmeister, J.: A review of modern treeline migration, the factors controlling it and the  
470 implications for Carbon Storage, *Journal of Mountain Science*, 18(2), 291–306, doi:10.1007/s11629-020-6221-1, 2021.

471 Hoch, G. and Körner, C.: Global patterns of mobile carbon stores in trees at the high-Elevation Tree Line, *Global Ecology*  
472 and *Biogeography*, 21(8), 861–871, doi:10.1111/j.1466-8238.2011.00731.x, 2011.

473 Huang, J.-G., Ma, Q., Rossi, S., Biondi, F., Deslauriers, A., Fonti, P., Liang, E., Mäkinen, H., Oberhuber, W., Rathgeber, C.  
474 B., Tognetti, R., Treml, V., Yang, B., Zhang, J.-L., Antonucci, S., Bergeron, Y., Camarero, J. J., Campelo, F., Čufar, K.,  
475 Cuny, H. E., De Luis, M., Giovannelli, A., Gričar, J., Gruber, A., Gryc, V., Güney, A., Guo, X., Huang, W., Jyske, T.,  
476 Kašpar, J., King, G., Krause, C., Lemay, A., Liu, F., Lombardi, F., Martinez del Castillo, E., Morin, H., Nabais, C., Nöjd,  
477 P., Peters, R. L., Prislan, P., Saracino, A., Swidrak, I., Vavrčík, H., Vieira, J., Yu, B., Zhang, S., Zeng, Q., Zhang, Y. and  
478 Ziacò, E.: Photoperiod and temperature as dominant environmental drivers triggering secondary growth resumption in  
479 northern hemisphere conifers, *Proceedings of the National Academy of Sciences*, 117(34), 20645–20652,  
480 doi:10.1073/pnas.2007058117, 2020.

481 Jevšenak, J. and Levanič, T.: DendroTools: R package for studying linear and nonlinear responses between tree-rings and  
482 daily environmental data, *Dendrochronologia*, 48, 32–39, doi:10.1016/j.dendro.2018.01.005, 2018.

483 Jevšenak, J.: Daily Climate Data reveal stronger climate-growth relationships for an extended European tree-ring network,  
484 *Quaternary Science Reviews*, 221, 105868, doi:10.1016/j.quascirev.2019.105868, 2019.

485 Jochner, M., Bugmann, H., Nötzli, M. and Bigler, C.: Tree growth responses to changing temperatures across space and  
486 time: A fine-scale analysis at the treeline in the Swiss alps, *Trees*, 32(2), 645–660, doi:10.1007/s00468-017-1648-x,  
487 2017.

488 Kirchhefer, A. J.: The influence of slope aspect on tree-ring growth of *Pinus sylvestris* L. in northern Norway and its  
489 implications for climate reconstruction, *Dendrochronologia*, 18, 27–40, 2000.

490 Knibbe, B.: Personal Analysis System for Tree-ring Research 5 - Instruction Manual, SCIEM, Vienna, Austria., 2013.

491 Kolář, T., Čermák, P., Oulehle, F., Trnka, M., Štěpánek, P., Cudlín, P., Hruška, J., Büntgen, U. and Rybníček, M.: Pollution  
492 Control enhanced spruce growth in the “Black Triangle” near the Czech–Polish border, *Science of The Total  
493 Environment*, 538, 703–711, doi:10.1016/j.scitotenv.2015.08.105, 2015.

494 Körner, C.: Alpine treelines functional ecology of the global high elevation tree limits, Springer, Basel, Switzerland., 2012.

495 Kuželová, H. and Treml, V.: Landscape-scale variability of air and soil temperature related to tree growth in the treeline  
496 ecotone, *Alpine Botany*, 130(1), 75–87, doi:10.1007/s00035-020-00233-8, 2020.

497 Körner, C. and Hiltbrunner, E.: Rapid advance of climatic tree limits in the eastern alps explained by on-site temperatures,  
498 *Regional Environmental Change*, 24(3), doi:10.1007/s10113-024-02259-8, 2024.

499 Körner, C. and Hiltbrunner, E.: The 90 ways to describe plant temperature, *Perspectives in Plant Ecology, Evolution and  
500 Systematics*, 30, 16–21, doi:10.1016/j.ppees.2017.04.004, 2018.

501 Körner, C. and Hoch, G.: A test of treeline theory on a montane Permafrost Island, Arctic, Antarctic, and Alpine Research,  
502 38(1), 113–119, doi:10.1657/1523-0430(2006)038[0113:atotto]2.0.co;2, 2006.

503 Körner, C. and Paulsen, J.: A world-wide study of high altitude treeline temperatures, *Journal of Biogeography*, 31(5), 713–  
504 732, doi:10.1111/j.1365-2699.2003.01043.x, 2004.

505 Körner, C.: The cold range limit of trees, *Trends in Ecology & Evolution*, 36(11), 979–989, doi:10.1016/j.tree.2021.06.011,  
506 2021a.

507 Körner, C.: The forest's nutrient cycle drives its carbon cycle, *Tree Physiology*, 42(3), 425–427,  
508 doi:10.1093/treephys/tpab170, 2021b.

509 Lenz, A., Hoch, G. and Körner, C.: Early season temperature controls cambial activity and total tree ring width at the Alpine  
510 treeline, *Plant Ecology & Diversity*, 6(3–4), 365–375, doi:10.1080/17550874.2012.711864, 2013.

511 Li, Y., Tian, D., Yang, H. and Niu, S.: Size-dependent nutrient limitation of tree growth from subtropical to cold temperate  
512 forests, *Functional Ecology*, 32(1), 95–105, doi:10.1111/1365-2435.12975, 2017.

513 Li, X., Liang, E., Camarero, J.J., Rossi, S., Zhang, J., Zhu, H., Fu, Y., Sun, J., Wang, T., Piao, S. and Peñuelas J.: Warming-  
514 induced phenological mismatch between trees and shrubs explains high-elevation forest expansion, *National Science  
515 Review*, 10, nwad182, <https://doi.org/10.1093/nsr/nwad182>, 2023.

516 Liebig, J.: *Die organische chemie in ihrer Anwendung auf Agricultur und Physiologie*, Vieweg, Braunschweig, Germany.,  
517 1840.

518 Liptzin, D., Sanford, R. L. and Seastedt, T. R.: Spatial patterns of total and available n and p at Alpine Treeline, *Plant and  
519 Soil*, 365(1–2), 127–140, doi:10.1007/s11104-012-1379-0, 2012.

520 Lu, X., Liang, E., Wang, Y., Babst, F. and Camarero, J.J.: Mountain treelines climb slowly despite rapid climate warming.  
521 *Global Ecology & Biogeography*, 30 (1), <https://doi.org/10.1111/geb.13214>, 2021.

522 Lucas, R. W., Klaminder, J., Futter, M. N., Bishop, K. H., Egnell, G., Laudon, H. and Höglberg, P.: A meta-analysis of the  
523 effects of nitrogen additions on base cations: Implications for plants, soils, and streams, *Forest Ecology and  
524 Management*, 262(2), 95–104, doi:10.1016/j.foreco.2011.03.018, 2011.

525 Lundqvist, S.-O., Seifert, S., Grahn, T., Olsson, L., García-Gil, M. R., Karlsson, B. and Seifert, T.: Age and weather effects  
526 on between and within ring variations of number, width and coarseness of tracheids and radial growth of young Norway  
527 spruce, *European Journal of Forest Research*, 137(5), 719–743, doi:10.1007/s10342-018-1136-x, 2018.

528 Mehlich, A.: Mehlich 3 soil test extractant: A modification of Mehlich 2 extractant, *Communications in Soil Science and  
529 Plant Analysis*, 15(12), 1409–1416, doi:10.1080/00103628409367568, 1984.

530 Mellert, K. H. and Ewald, J.: Nutrient limitation and site-related growth potential of Norway spruce (*Picea abies* [L.] karst) in  
531 the Bavarian alps, *European Journal of Forest Research*, 133(3), 433–451, doi:10.1007/s10342-013-0775-1, 2014.

532 Metelka, L., Mrkvica, Z. and Halászová, O.: Climate, in Krkonoše – nature, history, life, pp. 147–155, Baset, Prague., 2007.

533 Möhl, P., Mörsdorf, M. A., Dawes, M. A., Hagedorn, F., Bebi, P., Viglietti, D., Freppaz, M., Wipf, S., Körner, C., Thomas,  
534 F. M. and Rixen, C.: Twelve years of low nutrient input stimulates growth of trees and dwarf shrubs in the treeline  
535 ecotone, *Journal of Ecology*, 107(2), 768–780, doi:10.1111/1365-2745.13073, 2018.

536 Müller, M., Oelmann, Y., Schickhoff, U., Böhner, J. and Scholten, T.: Himalayan treeline soil and foliar C:N:P  
537 stoichiometry indicate nutrient shortage with elevation, *Geoderma*, 291, 21–32, doi:10.1016/j.geoderma.2016.12.015,  
538 2017.

539 Norby, R. J., Warren, J. M., Iversen, C. M., Childs, J., Jawdy, S. S. and Walker, A. P.: Forest stand and canopy development  
540 unaltered by 12 years of CO<sub>2</sub> Enrichment\*, *Tree Physiology*, 42(3), 428–440, doi:10.1093/treephys/tpab107, 2021.

541 Novotný, R., Lomský, B. and Šrámek, V.: Changes in the phosphorus and nitrogen status and supply in the young spruce  
542 stands in the Lužické, the jizerské and the Orlické Mts. in the Czech Republic during the 2004–2014 period, *European  
543 Journal of Forest Research*, 137(6), 879–894, doi:10.1007/s10342-018-1146-8, 2018.

544 Ols, C., Klesse, S., Girardin, M. P., Evans, M. E. K., DeRose, R. J. and Trouet, V.: Detrending climate data prior to climate–  
545 growth analyses in dendroecology: A common best practice?, *Dendrochronologia*, 79, 126094,  
546 doi:10.1016/j.dendro.2023.126094, 2023.

547 Oulehle, F., Urban, O., Tahovská, K., Kolář, T., Rybníček, M., Büntgen, U., Hruška, J., Čáslavský, J. and Trnka, M.:  
548 Calcium availability affects the intrinsic water-use efficiency of temperate forest trees, *Communications Earth & Environment*, 4(1),  
549 doi:10.1038/s43247-023-00822-5, 2023.

550 Paulsen, J. and Körner, C.: GIS-analysis of tree-line elevation in the Swiss alps suggests no exposure effect, *Journal of  
551 Vegetation Science*, 12(6), 817–824, doi:10.2307/3236869, 2001.

552 R Development Core Team: R: A language and environment for statistical computing, R Foundation for Statistical  
553 Computing, Vienna, Austria. 2023.

554 Rautio, P., Fürst, A., Stefan, K., Raitio, H., Bartels, U.: Part XII: Sampling and Analysis of Needles and Leaves, Version  
555 2020-3, In: UNECE ICP Forests Programme Co-ordinating Centre (ed.): Manual on methods and criteria for harmonized  
556 sampling, assessment, monitoring and analysis of the effects of air pollution on forests, Thünen Institute of Forest  
557 Ecosystems, Eberswalde, Germany. 2020.

558 Rathgeber, C. B., Rossi, S. and Bontemps, J.-D.: Cambial activity related to tree size in a mature silver-fir plantation, *Annals  
559 of Botany*, 108(3), 429–438, doi:10.1093/aob/mcr168, 2011.

560 Rathgeber, C. B., Santenoise, P. and Cuny, H. E.: Caviar: An R package for checking, displaying and processing wood-  
561 formation-monitoring data, *Tree Physiology*, 38(8), 1246–1260, doi:10.1093/treephys/tpy054, 2018.

562 Rossi, S., Anfodillo, T., Čufar, K., Cuny, H. E., Deslauriers, A., Fonti, P., Frank, D., Gričar, J., Gruber, A., Huang, J., Jyske,  
563 T., Kašpar, J., King, G., Krause, C., Liang, E., Mäkinen, H., Morin, H., Nöjd, P., Oberhuber, W., Prislan, P., Rathgeber,  
564 C. B. K., Saracino, A., Swidrak, I. and Treml, V.: Pattern of xylem phenology in conifers of cold ecosystems at the  
565 Northern Hemisphere, *Global Change Biology*, 22(11), 3804–3813, doi:10.1111/gcb.13317, 2016.

566 Rossi, S., Deslauriers, A. and Anfodillo, T.: Assessment of cambial activity and xylogenesis by microsampling tree species:  
567 An example at the alpine timberline, *IAWA Journal*, 27(4), 383–394, doi:10.1163/22941932-90000161, 2006a.

568 Rossi, S., Deslauriers, A. and Morin, H.: Application of the gompertz equation for the study of xylem cell development,  
569 *Dendrochronologia*, 21(1), 33–39, doi:10.1078/1125-7865-00034, 2003.

570 Rossi, S., Deslauriers, A., Anfodillo, T. and Carraro, V.: Evidence of threshold temperatures for xylogenesis in conifers at  
571 high altitudes, *Oecologia*, 152(1), 1–12, doi:10.1007/s00442-006-0625-7, 2006c.

572 Rossi, S., Deslauriers, A., Anfodillo, T., Morin, H., Saracino, A., Motta, R. and Borghetti, M.: Conifers in cold environments  
573 synchronize maximum growth rate of tree-ring formation with day length, *New Phytologist*, 170(2), 301–310,  
574 doi:10.1111/j.1469-8137.2006.01660.x, 2006b.

575 Rossi, S., Deslauriers, A., Gričar, J., Seo, J., Rathgeber, C. B., Anfodillo, T., Morin, H., Levanic, T., Oven, P. and Jalkanen,  
576 R.: Critical temperatures for xylogenesis in conifers of cold climates, *Global Ecology and Biogeography*, 17(6), 696–707,  
577 doi:10.1111/j.1466-8238.2008.00417.x, 2008.

578 Rousi, M., Possen, B. J., Ruotsalainen, S., Silfver, T. and Mikola, J.: Temperature and soil fertility as regulators of tree line  
579 Scots pine growth and survival—implications for the acclimation capacity of northern populations, *Global Change  
580 Biology*, 24(2), doi:10.1111/gcb.13956, 2017.

581 Shi, C., Schneider, L., Hu, Y., Shen, M., Sun, C., Xia, J., Forbes, B. C., Shi, P., Zhang, Y. and Ciais, P.: Warming-induced  
582 unprecedented high-elevation forest growth over the monsoonal Tibetan Plateau, *Environmental Research Letters*, 15(5),  
583 054011, doi:10.1088/1748-9326/ab7b9b, 2020.

584 Shi, H., Zhou, Q., He, R., Zhang, Q. and Dang, H.: Climate warming will widen the lagging gap of global treeline shift  
585 relative to densification, *Agricultural and Forest Meteorology*, 318, 108917, doi:10.1016/j.agrformet.2022.108917, 2022.

586 Speer, J. H.: *Fundamentals of Tree Ring Research*, University of Arizona Press, Tucson., 2010.

587 Stark, S., Kumar, M., Myrsky, E., Vuorinen, J., Kantola, A. M., Telkki, V.-V., Sjögersten, S., Olofsson, J. and Männistö, M.  
588 K.: Decreased soil microbial nitrogen under vegetation ‘shrubification’ in the subarctic forest–Tundra Ecotone: The  
589 potential role of increasing nutrient competition between plants and soil microorganisms, *Ecosystems*, 26(7), 1504–1523,  
590 doi:10.1007/s10021-023-00847-z, 2023.

591 Sullivan, P. F., Ellison, S. B., McNow, R. W., Brownlee, A. H. and Sveinbjörnsson, B.: Evidence of soil nutrient  
592 availability as the proximate constraint on growth of treeline trees in northwest Alaska, *Ecology*, 96(3), 716–727,  
593 doi:10.1890/14-0626.1, 2015.

594 Treml, V. and Banaš, M.: The effect of exposure on Alpine treeline position: A case study from the high sudetes, Czech  
595 Republic, *Arctic, Antarctic, and Alpine Research*, 40(4), 751–760, doi:10.1657/1523-0430(07-060)[treml]2.0.co;2, 2008.

596 Treml, V., Hejda, T. and Kašpar, J.: Differences in growth between shrubs and trees: How does the stature of woody plants  
597 influence their ability to thrive in cold regions?, *Agricultural and Forest Meteorology*, 271, 54–63,  
598 doi:10.1016/j.agrformet.2019.02.036, 2019.

599 Treml, V., Kašpar, J., Kuželová, H. and Gryc, V.: Differences in intra-annual wood formation in *Picea abies* across the  
600 treeline ecotone, *Giant Mountains, czech republic, Trees*, 29(2), 515–526, doi:10.1007/s00468-014-1129-4, 2014.

601 Tumajer, J., Kašpar, J., Kuželová, H., Shishov, V. V., Tychkov, I. I., Popkova, M. I., Vaganov, E. A. and Treml, V.: Forward  
602 modeling reveals multidecadal trends in cambial kinetics and phenology at treeline, *Frontiers in Plant Science*, 12,  
603 doi:10.3389/fpls.2021.613643, 2021.

604 Zeng, Q., Rossi, S. and Yang, B.: Effects of age and size on xylem phenology in two conifers of northwestern China,  
605 *Frontiers in Plant Science*, 8, doi:10.3389/fpls.2017.02264, 2018.

606 Zhou, T., Du, W., Wang, J., Zhang, L., Gao, J., Shi, N., Wang, L., Wu, Y. and Tian, B.: Divergent responses of plant  
607 functional traits and biomass allocation to slope aspects in four perennial herbs of the Alpine Meadow Ecosystem,  
608 *Frontiers in Plant Science*, 14, doi:10.3389/fpls.2023.1092821, 2023.

609 Zweifel, R., Sterck, F., Braun, S., Buchmann, N., Eugster, W., Gessler, A., Häni, M., Peters, R. L., Walther, L., Wilhelm,  
610 M., Ziemińska, K. and Etzold, S.: Why trees grow at night, *New Phytologist*, 231(6), 2174–2185,  
611 doi:10.1111/nph.17552, 2021.

612